The sperm hook in house mice: a functional adaptation for migration and self-organised behaviour

Short title: Mouse sperm behaviour in the female reproductive tract

Heungjin Ryu[1,2]*†, Kibum Nam[1]†, Byeong Eun Lee[3]†, Yundon Jeong[1]†, Seunghun Lee[1], Jeongmo Kim[1], Young-Min Hyun[4], Jae-Ick Kim[3]*, Jung-Hoon Park[1]*

1. Department of Biomedical Engineering, Ulsan National Institute of Science and Technology; Ulju-gun, Ulsan, 44919, Republic of Korea

2. Department of Social Informatics, Kyoto University; Sakyo-ku, Kyoto 606-8501, JAPAN

3. Department of Biological Sciences, Ulsan National Institute of Science and Technology; Ulju-gun, Ulsan, 44919, Republic of Korea

4. Department of Anatomy, Yonsei University College of Medicine, Seoul, 03722, Republic of Korea

*Corresponding authors. Heungjin Ryu, Jae-Ick Kim, Jung-Hoon Park

Corresponding authors' email**:** ryu.heungjin.26v@kyoto-u.jp; jikim220@unist.ac.kr; jh.park@unist.ac.kr

Abstract

In most murine species, spermatozoa exhibit a falciform apical hook at the head end. The function of the sperm hook is not yet clearly understood. In this study, we investigate the role of the sperm hook in the migration of spermatozoa through the female reproductive tract in *Mus musculus* (C57BL/6), using a deep tissue imaging custom-built two-photon microscope. Through live reproductive tract imaging, we found evidence indicating that the sperm hook aids in the attachment of spermatozoa to the epithelium and facilitates interactions between spermatozoa and the epithelium during migration in the uterus and oviduct. We also observed synchronised sperm beating, which resulted from the spontaneous unidirectional rearrangement of spermatozoa in the uterus. Based on live imaging of spermatozoa-epithelium interaction dynamics, we propose that the sperm hook plays a crucial role in successful migration through the female reproductive tract by providing anchor-like mechanical support and facilitating interactions between spermatozoa and the female reproductive tract in the house mouse.

Keywords: migration kinetics, mouse, sperm hook, sperm train, sperm migration, two-photon microscope, female reproductive tract

Introduction

Since the pioneering work by Parker (Parker, 1970), postcopulatory sexual selection has been recognised as an important driving force that shapes male sperm and female reproductive track

characteristics. Post-copulatory sperm competition over gamete and cryptic female choice are equivalent to male-male competition and female choice in the pre-copulatory sexual selection. Sperm competition occurs when spermatozoa from more than one male coincide within the female reproductive tract in a time window where they have a chance to fertilize the same egg (Parker, 1970). The evolutionary consequences of the sperm competition for the male traits, including baculum complexity, sperm shape and behaviour, are demonstrated in a wide range of animals from insects to mammals (Anderson et al., 2005; Lange et al., 2013; André et al., 2020). Such male adaptations secure sperm delivery to the female reproductive tract and influence sequential mating of the already mated female with other males. Cryptic female choice is a more complicated process to define as it is achieved at the various stages of the post-mating fertilization process that also occurs inside the female reproductive tract. However, post-copulatory cryptic female choice is evident where a female can exert an influence on ejaculates or even fertilised eggs that can influence male's reproductive success (Eberhard, 1996; Firman et al., 2017; Roberts et al., 2012).

Postcopulatory sexual selection results in co-evolution of the male and female traits that impact the reproductive strategies of the opposite sex (Eberhard and Lehmann, 2019; Greff and Parker, 2000). For example, copulatory plugs formed by male semen hinder sequential mating of the female with a second male and diminish the reproductive outcome of the second male (Mangels et al., 2016; Sutter and Lindholm, 2016). Females, on the other hand, by removing the copulatory plug, can counteract male strategy (Koprowski, 1992). When fluid in female reproductive tract is spermicidal, male seminal fluid neutralises the spermicidal medium and secures sperm survival inside the female reproductive tract (Holman and Snook, 2008, 2006).

Among mammals, rodent species exhibit various sperm morphological and behavioural characteristics. A notable morphological feature of murine sperm is the apical hook resulting in an asymmetrical falciform head shape that are found in most of the murine rodents (Breed, 2004; Roldan et al., 1992). The functional significance of the sperm hook that causes head asymmetry is still under debate in the field of mouse reproductive ecology. Currently, two main hypotheses attempt to explain the function of the sperm hook. One is that the sperm hook plays a crucial role in sperm competition by aiding sperm linkage (sperm train formation) that enhances straighter and faster sperm forward progression – the sperm cooperation hypothesis (Fisher and Hoekstra, 2010; Moore et al., 2002). The other hypothesis is that the sperm hook facilitates sperm-epithelium interactions in the female reproductive tract, playing a significant role in sperm migration – the migration hypothesis (Smith and Yanagimachi, 1990; Firman and Simmons, 2009). The sperm cooperation hypothesis is supported by the pioneering discovery of sperm linkage known as sperm trains (Moore et al., 2002) and suggests that sperm trains facilitate faster or straighter sperm swimming (Fisher and Hoekstra, 2010; Moore et al., 2002). However, other studies could not find supporting evidence of sperm cooperation by the sperm train or morphological changes in sperm hooks concerning the degree of sperm competition (Firman and Simmons, 2009; Hook et al., 2021). These researchers rather suggest that the sperm hook plays a crucial role in sperm migration by interacting with epithelia in the female reproductive tract.

Since thick muscle layers comprise the outer part of rodent female reproductive tract, direct observation of spermatozoa inside the female reproductive tract is a challenging feat. Therefore previous studies focused on the oviduct where muscle layers are thin and transparent, using

brightfield, fluorescence or confocal microscopy (Ishikawa et al., 2016; Qu et al., 2021; Suarez, 1987). In this study, we developed an ex-vivo observation system based on a custom-built two-photon microscope (Fig. S1). This system enables the observation of spermatozoa and their behaviour inside the live female reproductive tract. While two-photon microscopy is currently the method of choice for live imaging of deep tissues (Helmchen and Denk, 2005; Benninger and Piston, 2013; Keller, 2013), it has seldom been used for studying animal reproductive ecology. Here, we demonstrate high-resolution deep-tissue imaging that allows us to observe and track sperm movement inside the female reproductive tract, including the uterus, to realise real-time tracking of spermatozoa and their migration.

Using this technology, we report newly discovered sperm behaviour and aggregation patterns that suggest various roles of the sperm hook in sperm migration inside the female reproductive tract. Based on live imaging of sperm dynamics inside the live female reproductive tract, we provide new observations and insights that suggest functions of the sperm hook that help sperm migration and cooperation. With our new observation system and results, we hope to contribute to the field of postcopulatory sexual selection in rodents by advancing methodological progress and stimulating discussion and future research on the function of sperm hook in murine rodents.

Results

To observe mouse sperm behaviour in the female reproductive tract, we mated wild-type *Mus musculus* (C57BL/6) females with transgenic male mice (Tables S1; S2) that express DsRed at the sperm mid-piece (mitochondria) and eGFP in the sperm acrosome (Hasuwa et al., 2010). The female mice were euthanised between 0.5- and 3-hours post-mating, and their reproductive tract along with copulatory plug was excised and transferred to a sterilized Petri dish. We then conducted *ex-vivo* imaging of the live reproductive tract using our two-photon microscope (Fig. S1). Figure 1A is a diagram of the female reproductive tract that labels the name of each part of the tract. All observations were typically completed within 3 hours and did not exceed 6 hours post-euthanasia. Despite this observation period being longer than recommended for conventional rat transplantation surgery (Díaz-García et al., 2013), we noted live uterine movements throughout the entire observation period. When samples were transferred to incubators preheated to 37°C with 5% CO_2 following observation, uterine movement persisted even 24 hours post-excision. We used Fiji (Schindelin et al., 2012) and R 4.3.3 (R Core Team, 2024) for image processing and statistical analysis.

The role of sperm hook in migration inside the uterus

We first observed sperm movement in the uterus, where most ejaculated spermatozoa are located and initial sperm selection occurs. In the uterus, we observed vigorous fluid flow caused by uterine contraction and relaxation. Consequently, most spermatozoa in the uterus were carried by this flow, adhering to the inherent flow dynamics within the uterus (Movie S1A). However, when the flow temporarily ceased, spermatozoa located near the uterine wall exhibited greater activity (Movie S1B, C). When a spermatozoon encounters the uterine wall (epithelium) during migration, the sperm hook interacted with the wall and acts as a pivot (Yu et al., 2023) that influences the direction of sperm travel (Figure 1B, C). Movie S2A shows two distinct types of sperm movement when transitioning from the uterus volume to the uterine wall: pro-wall-hook

and anti-wall-hook directional movement (Figure 1C). Upon reaching the uterine wall, instead of randomly deflecting in various directions, sperm preferentially altered their heading direction such that their apical hook would face the uterine wall (pro-wall-hook direction).

To test whether the hook influences the direction of migration, we tracked spermatozoa that travelled from the uterus volume to the wall in sequentially acquired images. We found that 52 out of 63 spermatozoa (82.54%) changed their migration direction towards the pro-wall-hook direction after reaching the uterine wall (Figure 1D). The remaining 11 spermatozoa followed the anti-wall-hook direction. A binomial test confirmed that this tendency was statistically significant (one-tailed, $p < .001$, 95% CI: 0.73, 1.00). Furthermore, when spermatozoa migrated along the uterine wall, they exhibited a tapping-like behaviour in which spermatozoa tapped their hook against the epithelium when oriented in a pro-wall-hook direction (Movie S2B). In contrast, when the sperm hook faces the luminal space, spermatozoa could not migrate along the wall and their migration trajectories followed the anti-wall-hook direction, resulting in movement away from the wall (Figure 1D; Movie S2A). In addition to the advantage in straighter trajectories, fluid flows are slower at the wall than at the centre of the lumen in the uterus (Zaferani et al., 2019). Therefore migration along the uterine wall will help spermatozoa to reach the entrance of the intramural utero-tubal junction (UTJ), also called colliculus tubarius (CT), where one of the most important sperm selection processes takes place (Nakanishi et al., 2004; Qu et al., 2021).

Sperm anchoring and migration kinetics in the uterus

We observed that the sperm head was attaching to the epithelium of the CT and uterus (Movie S3A, B) when spermatozoa reached the CT. The sperm hook was affixed to the epithelium, thereby securing the spermatozoa on the epithelia. We defined this securing of the spermatozoa on the epithelia by the sperm hook as an anchor-like function of the hook (Movie S3A, B). This anchoring also helped prevent spermatozoa from being swept away by mucosal flow (Figure 1E; Movie S3B). When spermatozoa attached to the CT and squeezed through other spermatozoa by hooking, the apical hook always faced the epithelium (Figure 1F; Movie S3A). Once spermatozoa successfully clung onto the CT, anchoring to the epithelia prevented them from being pushed out by competing spermatozoa or from being swept away by fluid flow (Movie S3B).

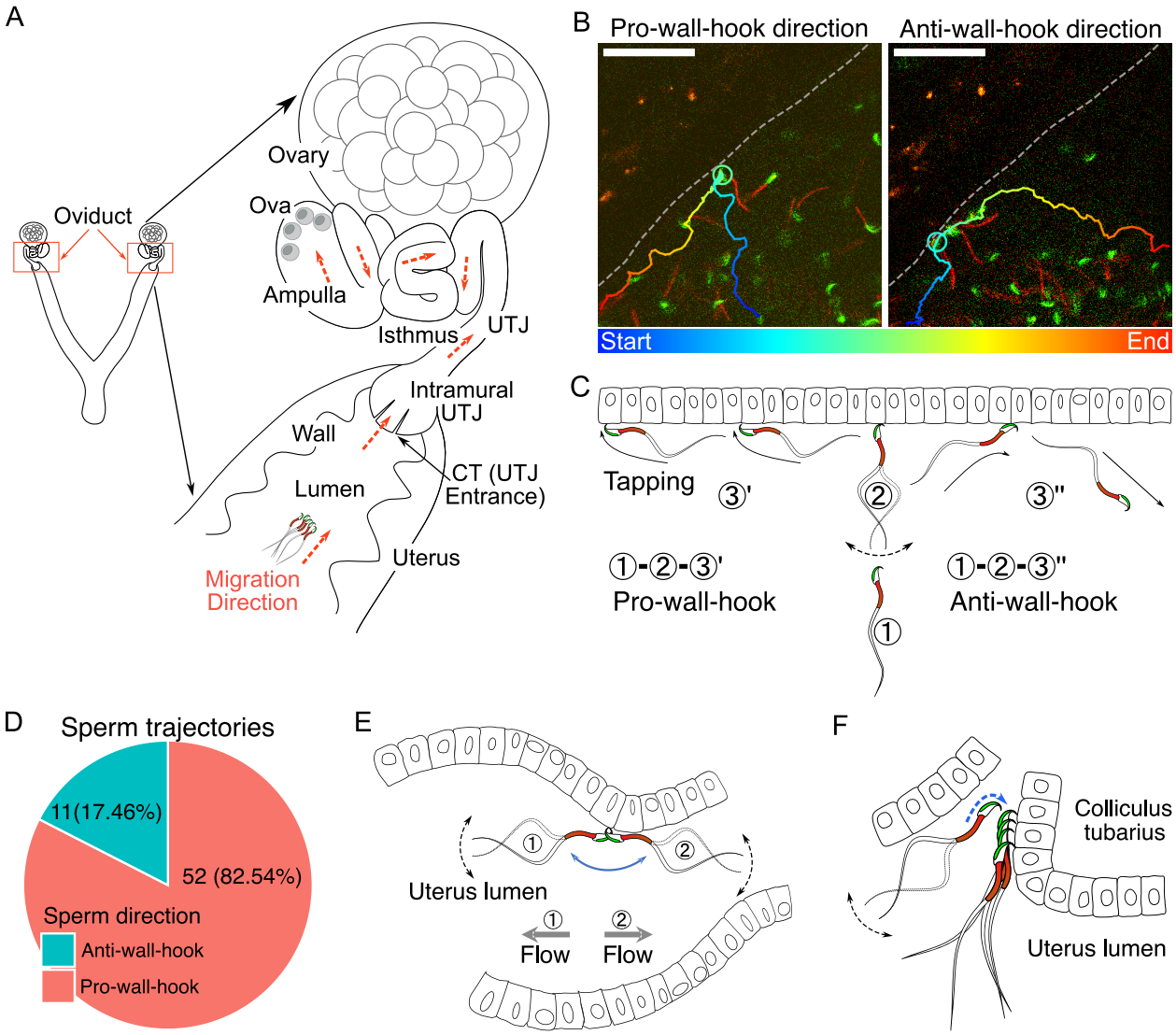

Figure 1. The structure of female reproductive tract and various sperm behaviours and interactions with epithelia in the uterus. (**A**) An illustration of the female reproductive tract and sperm migration direction (arrows in orange colour) inside the tract. Ova (egg cells) are in the ampulla. (**B**) Spermatozoa alter their travel direction based on their head orientation upon reaching the uterine wall (sperm hook functions as a pivot, Movie S2A). Left image shows a sperm trajectory exhibiting pro-wall-hook direction, and the right image shows anti-wall-hook direction. The trajectory is depicted in colours representing different time points. Dashed lines are guides to the eye to visualize the uterus wall. Scale bar: 50 µm. (**C**) Sperm moving direction changes over time when they reach the uterine epithelia. Numbers indicate sequences of sperm movement. (1) During sperm migration, they reach the uterine wall. (2) After reaching the uterine wall, they beat several times while facing their head towards the uterine wall. (3) Sperm beating results in a change in sperm orientation (1 to 3′: pro-wall-hook, 1 to 3″: anti-wall-hook). The pro-wall-hook orientation coincides with sperm travelling along the wall and the anti-wall-hook orientation coincides with sperm moving away from the wall. (**D**) When spermatozoa reach the uterine wall, their trajectories predominantly follow the pro-wall-hook direction, where the sperm hook is directed towards the uterine wall. (**E**) The sperm hook assists a spermatozoon in anchoring to the epithelia (hook as an anchor). This anchoring facilitates sperm

attachment to the uterine and UTJ epithelium and prevents spermatozoa from being swept away by internal flow caused by peristaltic movement. (**F**) The sperm hook and thin sperm head aid spermatozoa in squeezing through the sperm-crowded UTJ entrance (CT) and attaching to the epithelium by acting as an anchor (Movie S3). Note that in our experiments, we do not observe the principal and terminal pieces of spermatozoa due to a lack of fluorescence in our animal model. The observed acrosome and midpiece are shown coloured in the schematic figures.

To compare sperm migration kinetics during sperm swimming relative to their distance from the uterine wall, we tracked sperm migration trajectories by employing the TrackMate plugin in ImageJ (Ershov et al., 2022; Tinevez et al., 2017). After successful tracking using the customised tracking option in TrackMate, we computed various sperm kinetic parameters. These parameters included the curvilinear velocity (VCL), straight-line velocity (VSL), and linearity of forward progression (LIN), which are commonly used in computer-assisted sperm analysis, CASA (Amann and Waberski, 2014). Briefly, VCL was calculated as the total distance travelled divided by total travel time, VSL as the distance between initial and final positions of the sperm trajectory divided by total travel time, and LIN as the ratio of VSL to VCL, which can range from 0 to 100%, with 100% representing a perfectly straight line. We also introduced a new kinetic parameter called straight line-to-sideward movement ratio (SWR), defined as track displacement of a sperm trajectory divided by maximum sideward movement distance. Refer to Fig. S2A, B for our definition of the uterus wall and a schematic description of the sperm migration kinetic parameters, as well as Methods for more details.

Our sperm tracking analysis revealed that spermatozoa located close to the uterine wall moved faster, exhibiting higher VCL and VSL (Figure 2A; Table S3; Movie S1B, C). However, LIN and SWR did not significantly vary depending on sperm's distance from the uterus wall (Figure 2B). In contrast to the non-significant changes in LIN and SWR relative to the distance from the uterine wall, when spermatozoa swam parallel to the wall, they not only moved faster (higher VCL and VSL; Figure 2A), but also followed a straighter path (higher LIN and SWR; Figure 2B). Given that the internal fluid flow around the uterine wall is slower (Zaferani et al., 2019), and considering the hydrodynamic factors that attract spermatozoa to the wall when swimming near it (Alvarez et al., 2014; Elgeti et al., 2010), migration along the wall would be an efficient strategy for sperm movement within the uterus. We also examined the impact of both individual males (coded as 'Male ID') and females (coded as 'Date') on the sperm kinetic parameters in all models by visualising the effects of these two random variables (Fig. S3). We confirmed that the effects of the two random variables were consistent across all significant models, indicating validity of our model estimations.

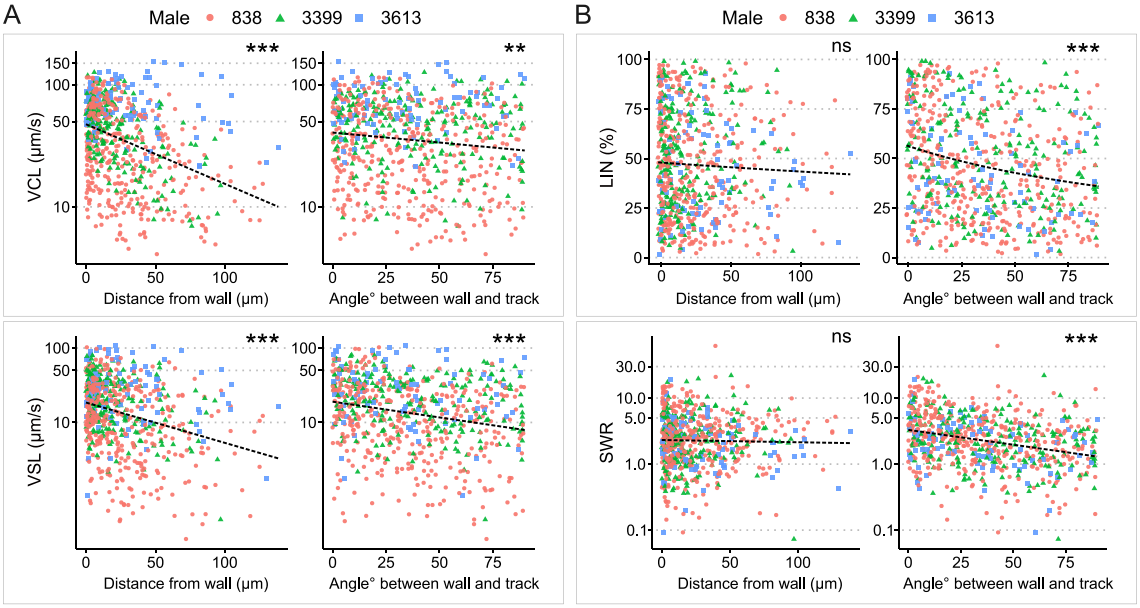

Figure 2. Analysis of sperm kinetic parameters relative to the distance and angle between the sperm trajectory and uterine wall. (**A**) Both VCL (top) and VSL (bottom) decreased with an increase in the distance between the sperm trajectory and the uterine wall. Similarly, VCL and VSL decreased as the angle between the sperm trajectory and uterine wall increased. (**B**) The distance between the sperm trajectory and uterine wall did not significantly affect LIN (top left) and SWR (bottom left). However, both LIN and SWR decreased when the angle between the sperm trajectory and uterine wall increased. Data from different males are represented in different colours and shapes. The dotted lines indicate regression lines from simple regressions to aid visual interpretation. Check model estimates for more details and precise interpretation of the models (Table S3; Fig. S3A, B). The y-axis of each figure is displayed in log-scale except for LIN. Images for sperm tracking were acquired around the area labelled as 'Wall' in the uterus in Figure 1A. Sperm trajectories used in this analysis are presented in Movie S1B. The effect of the two random variables (males and females) are visualised in Fig. S3.

Structure of UTJ and sperm behaviour at the entrance of intramural UTJ (CT)

Upon sacrificing and optical clearing the tissue, we confirmed that the entrance to the intramural UTJ (CT) in the uterus consists of nearly closed narrow gaps between mucosal folds (Figure 3A). These narrow gaps extended to about 100 μm deeper from the entrance (Movie S4A, B), and only a few spermatozoa could pass through a gap at a time (Figure 3A; Movie S4C). We were not able to find evidence of passive sperm carriage, such as upsuck-like sperm carriage (Baker and Bellis, 1993), caused by peristaltic movement from the uterus into the UTJ in real-time live images (Movie S5A). Therefore, we concluded that fluid flow induced by uterine and oviduct contraction is not a major driving force for sperm entry to the UTJ through the CT.

This conclusion raises a question about how spermatozoa enter the UTJ through the CT if the UTJ entrance is nearly closed. We found head-directional sliding of spermatozoa in the almost closed inter-luminal spaces between the uterus and intramural UTJ (Movie S5B). We did not observe any sliding of spermatozoa that directs to the tail-direction. This one-directional head-forward sliding in a very narrow inter-luminal space suggests a role of the sperm hook as an

anchor that prevents backward slipping by the squeezing movement from the contraction of the uterus. Such one-directional sliding is also a plausible way of sperm migration from the uterus to UTJ through the narrow gap at the CT. We also observed that when muscle contraction and relaxation occurred at the uterus and oviduct, the surfaces of two confronting mucosal folds in intramural UTJ slid against each other in opposite directions (Figure 3B; Movie S5B). Such an opposite directional movement of mucosal folds, for example, will occur when the uterus bends to the left due to muscle contraction on its left side and relaxation of its right side (Fig. S4). As shown in Movie S5B, the opposite movement of mucosal folds makes space between mucosal folds at the CT, providing an opportunity for nearby attached spermatozoa to enter the intramural UTJ (Fig. S4). Although application of further experimental approaches will be necessary, occasional fluctuations in the size of the luminal space between mucosal folds, caused by peristaltic movements, together with the head-directional sliding of the spermatozoa, may provide an opportunity for spermatozoa to pass through the CT.

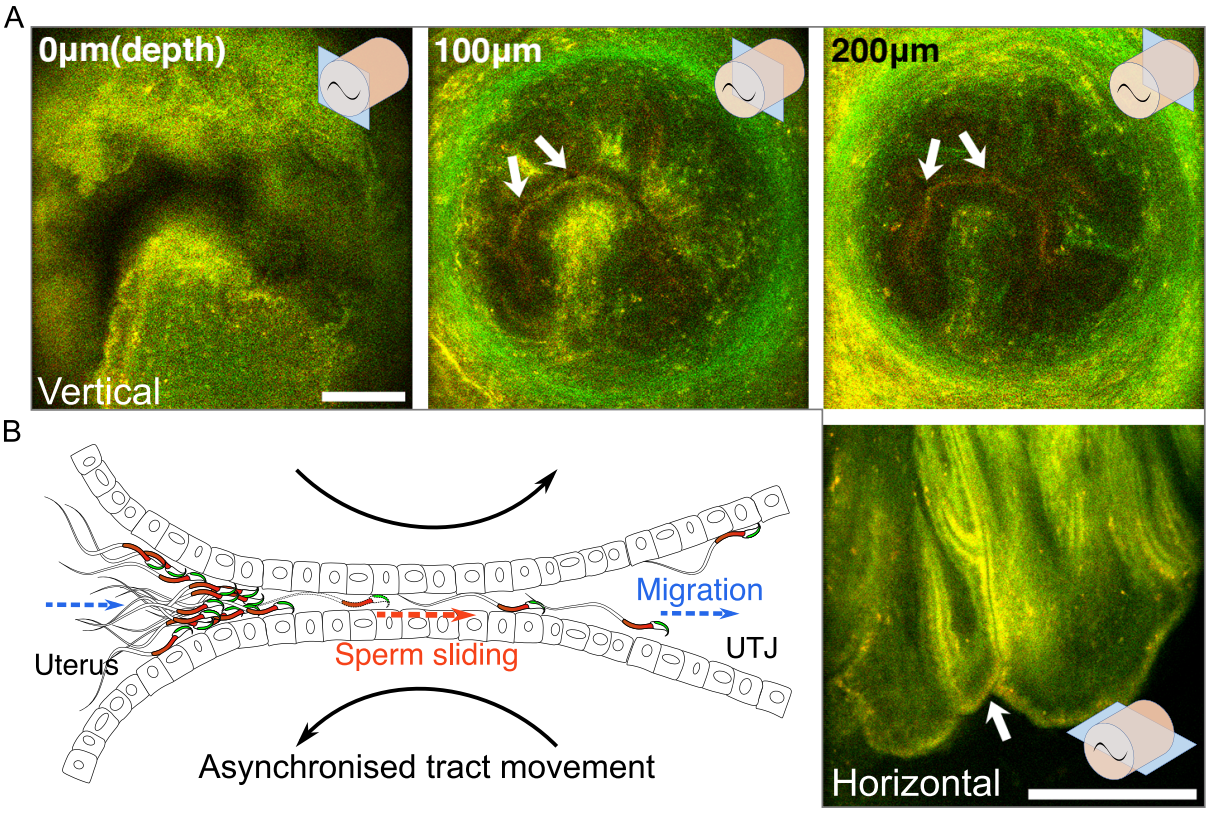

Figure 3. The structure of the entrance of intramural UTJ and sperm passage. (**A**) The upper three images are the vertical view of the CT (entrance to the UTJ) of the intramural UTJ from an unmated female. The bottom right image is a horizontal view of the intramural UTJ. There are only a few small gaps, indicated by arrows, between mucosal folds, which control sperm migration into the UTJ from the uterus (Movie S4). Illustrations at upper and lower right conners indicate imaging planes (blue rectangles) and the intramural UTJ (orange cylindrical structure) with the CT (black tilde). Scale bar: 100 μm, Arrow line thickness: 10 μm for top three images, 5 μm right bottom image. (**B**) Asynchronised movement of mucosal folds (sliding against each other) at the CT due to uterine and UTJ contractions enable spermatozoa to slide into the intramural UTJ from the uterus (Movie S5). Two dashed arrows (in blue) indicate the direction of sperm migration from the uterus to the UTJ, and

the dashed arrow in the centre (in orange) indicates the direction of sperm sliding in the intramural UTJ. The two curved black arrows indicate asynchronised (opposite) movement of confronting mucosal folds in the intramural UTJ.

We also observed unidirectional sperm clustering as a result of spontaneous sperm re-arrangement during sperm beating along the uterine wall (Figure 4A and Movie S6A, B). Such unidirectional sperm clustering and their successive beating resulted in synchronised sperm beating on some occasions (sperm self-organising behaviour). We also found such self-organised sperm behaviour on a large scale at the CT in which most of the clustered spermatozoa at the entrance of the intramural UTJ (CT) exhibited synchronised beating (Figure 4B; Movie S7). The synchronised sperm beating was observed to generate fluid flows strong enough to prevent other spermatozoa from attaching to the CT or directly push out other spermatozoa, thereby preventing other spermatozoa from entering the UTJ (Movie S6; S7).

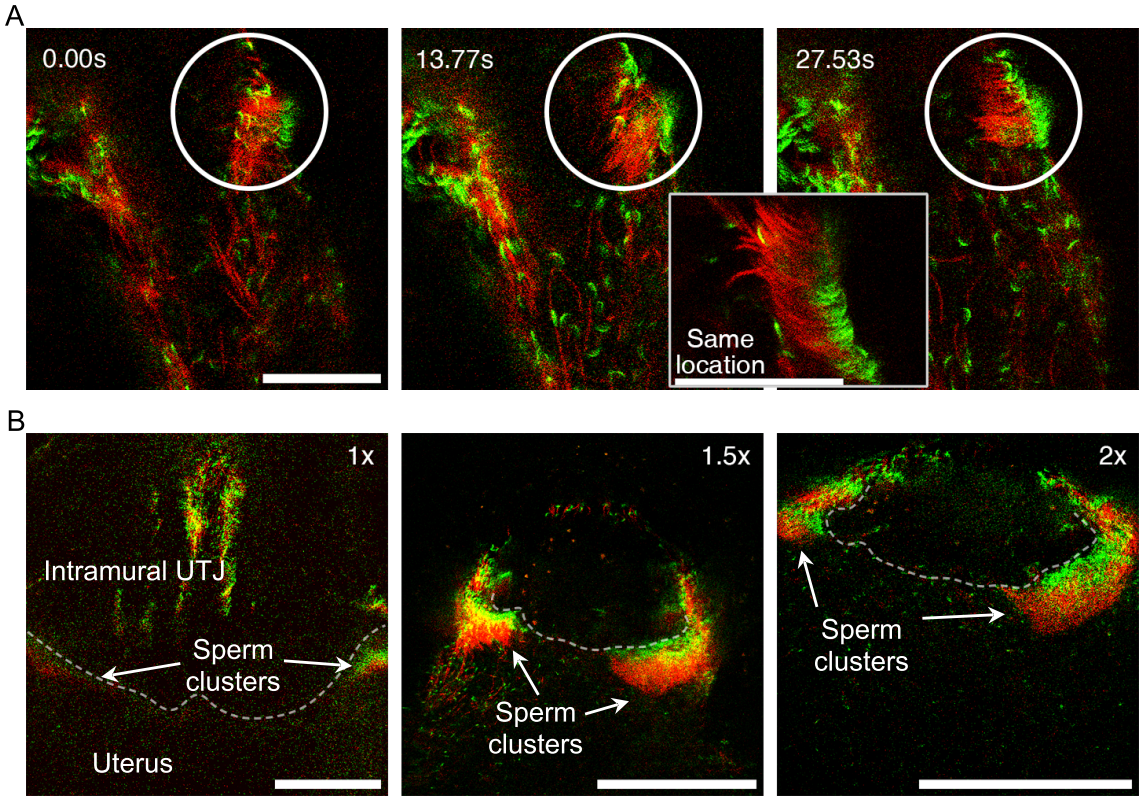

Figure 4. Self-organised sperm behaviour at CT inside the uterus. (**A**) The apical shape of the sperm head, due to the sperm hook, results in head asymmetry. This asymmetrical falciform head shape may facilitate sperm re-arrangement and clustering at uterine wall (Movie S6). The circle highlights spermatozoa undergoing unidirectional re-arrangement over time. The elapsed time after the first frame is shown in the upper left of the images. The right lower zoom-in inset shows an instant of synchronised motion and unidirectional re-arrangement. Scale bar: 50 µm. (**B**) Unidirectional sperm clustering at the entrance of the intramural UTJ (CT, indicated by a dashed line) is marked with arrows. Such large sperm clustering resulted in synchronised sperm beating at the CT (Movie S7). Scale bar: 200 µm. Note that due to a lack of fluorescence, the principal and terminal pieces of sperm tails are not seen in the images.

Sperm linkage and their migration kinetics

Unlike the sperm trains found in wood mice (*Apodemus sylvaticus;* Moore et al., 2002) and deer mice (*Peromyscus maniculatus;* Fisher and Hoekstra, 2010), most of the spermatozoa in this study did not form functional sperm trains (linked spermatozoa) (Figure 5A; Movie S8). Active sperm linkage or clusters were indeed observed but were rare (only 3 identifiable cases during over100 hours of imaging). For the house mouse, the observed sperm trains did not move faster or slower than unlinked single spermatozoa (Figure 5B; Movie S8). Their VCL, VSL, and LIN were not faster nor higher than those of unlinked single spermatozoa as shown in Figure 5B. Although their SWR may be higher than that of unlinked single spermatozoa, due to the rare number of observed events, further experiments will be necessary to clarify whether the sperm train formation is advantageous in the house mouse.

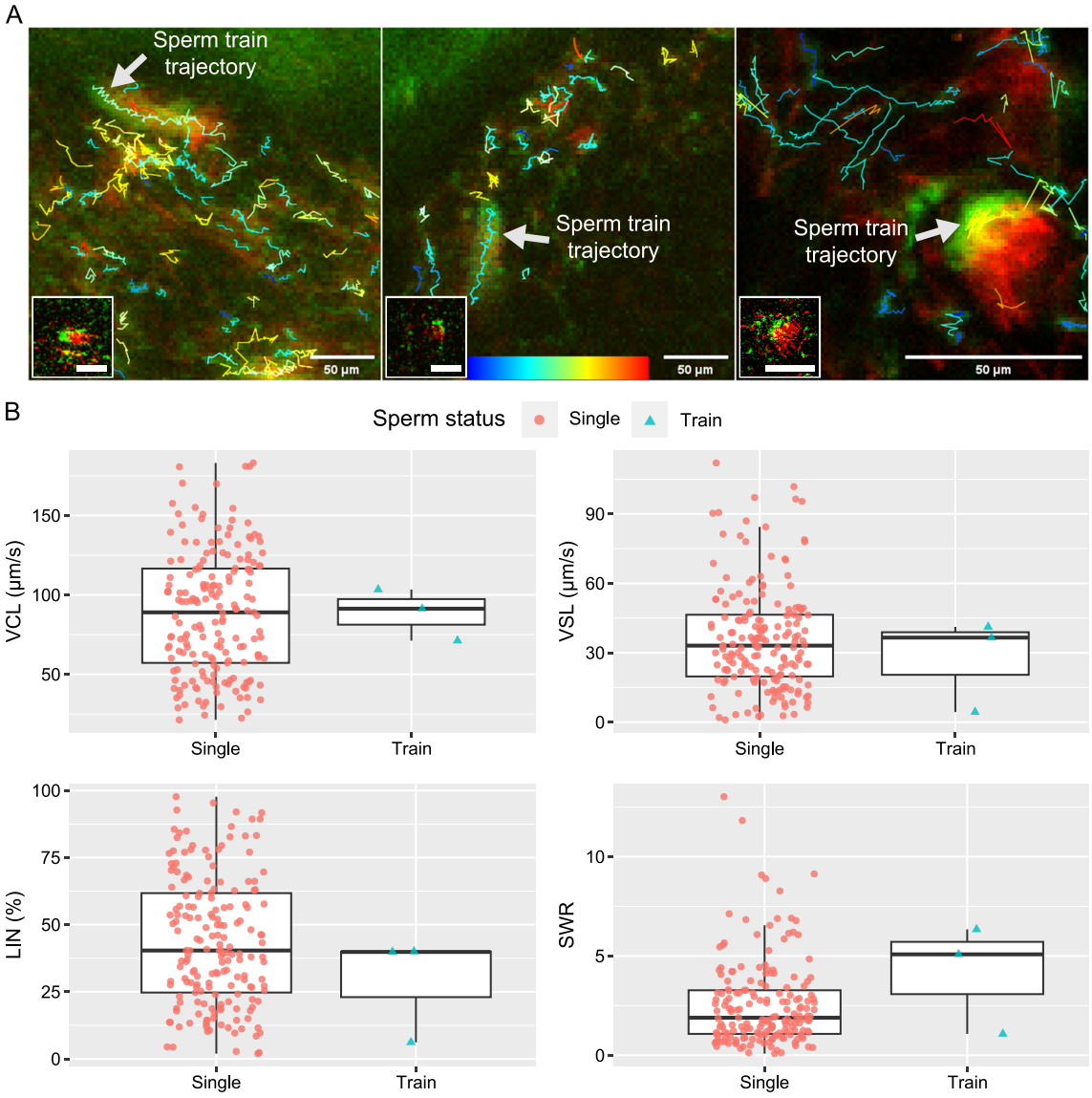

288 **Figure 5. Comparative trajectories and kinetics of linked spermatozoa (sperm trains) and**
289 **unlinked single spermatozoa** (**A**) The projected images, comprising 60 frames, depict the trajectories
290 of sperm trains and unlinked single spermatozoa. Each of the images in the lower left corner shows a
291 sperm train that was traced. Movie S8 shows how the three traced sperm trains are moving. The colour
292 bar located at the bottom centre represents the VCL of each sperm trajectory, with blue indicating
293 slower speeds and red indicating faster speeds. (**B**) The boxplots, which include individual data points,
294 represent the kinetic parameters of the sperm trains and unlinked single spermatozoa. The parameters,
295 including curvilinear velocity (VCL), straight-line velocity (VSL), linearity of forward progression
296 (LIN), and straight line-to-sideward movement ratio (SWR), were computed using images of 100x100
297 pixels that contained a sperm train. The three sperm trains that were traced did not exhibit a faster
298 VCL or VSL, nor a higher LIN. However, it is still possible that the SWR is higher in the sperm train.
299 The lines within the boxes represent the medians, and the whiskers represent 1.5 times the interquartile
300 ranges, and the symbols show the individual data points.

301

302 ***Sperm migration and accumulation in the oviduct***

303 After entering the UTJ, spermatozoa continued migration through the narrow UTJ lumen. In the
304 UTJ, spermatozoa interact with epithelia with their hook and penetrate their thin head into a
305 narrow space (Movie S9A). Contraction of the UTJ reduced the width of the UTJ lumen and
306 prevented sperm migration (Movie S9B). However, some spermatozoa could pass through the
307 narrow luminal space by putting their thin hook (Figure 6A, B; Movie S9B). During UTJ lumen
308 contraction, both swimming and beating of spermatozoa therein were physically suppressed.
309 When the UTJ lumen dilates, the suppressed spermatozoa started beating and swimming again
310 (Figure 6C; Movie S9B). We also found sperm accumulations in the oviduct, including UTJ and
311 isthmus (Figure 6D). However, as these sperm accumulations were arranged irregularly and
312 consisted of spermatozoa that were mostly acrosome reacted and inactive, they were considered
313 inactive entangled spermatozoa rather than active linked spermatozoa (or sperm trains). These
314 entangled spermatozoa filled the narrow oviductal lumen, creating an obstruction for the
315 migration of other spermatozoa (Movie S9C). If sperm hook facilitates such entanglement of
316 inactive spermatozoa in the UTJ and isthmus, it can play a role in sperm competition by
317 obstructing migration of the other spermatozoa including those from a second male.

318 Sperm beating rates of the epithelia-attached spermatozoa were observed to change over time
319 according to the changes in widths of the UTJ lumen (Movie S10). Although such a change in
320 beating rates may simply reflect luminal flow speed or luminal width related to physical space
321 for beating, it may also assist in attaching spermatozoa to the epithelium by providing propulsive
322 forces (Kantsler et al., 2014). Fluid flow in the UTJ and isthmus can damage unattached
323 spermatozoa, particularly when they get entangled with inactive entangled spermatozoa that are
324 moving back and forth by the flow (Movie S9C). If such beating prevents epithelium-attached
325 spermatozoa being swept away by the flow, sperm beating corresponding to the fluid flow will
326 be advantageous. The oviductal fluid gradually flows upward while continuously repeating back-
327 and-forth directional changes and such flow is assumed to aid sperm migration from UTJ to
328 ampulla (Hino and Yanagimachi, 2019). However, given our observation of resistant (anchoring)
329 behaviour of spermatozoa to the flow in the UTJ, passive sperm transfer may not always be
330 beneficial for healthy spermatozoa. Additionally, such passive transfer can cause physical

damage to the spermatozoa by the collision with other entangled spermatozoa or epithelia of the narrow lumen. Further experiments will be necessary to clarify the role of the rapid upward flow in the oviduct in the fertilization process in mice.

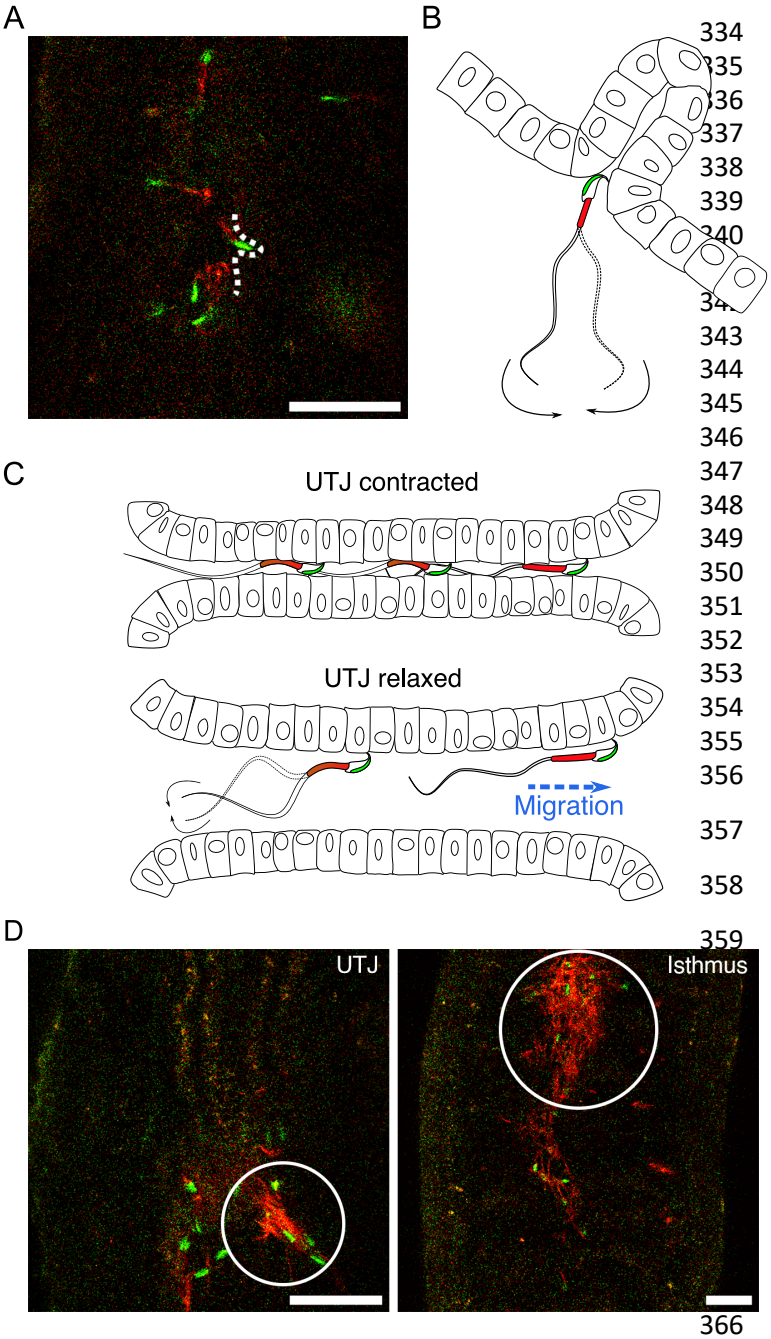

Figure 6. Sperm migration through narrow luminal space in UTJ and various sizes of accumulated sperm in the oviduct. (**A** and **B**) Spermatozoa can penetrate narrow space with their thin head and anchor their hook when they pass through the narrow gaps between mucosal folds during migration in the UTJ (Movie S9A). Scale bar: 50 µm. (**C**) Spermatozoa can only migrate through the UTJ when the luminal space is extended due to oviductal contraction and relaxation in the UTJ. (**D**) Entangled spermatozoa in the oviduct, including the UTJ and isthmus, were predominantly made up of inactive acrosome reacted spermatozoa. These entangled spermatozoa obstruct the migration of other active spermatozoa and can cause damage to live spermatozoa. Scale bar: 50 µm.

Discussion

Our real-time deep tissue imaging enabled by two-photon microscopy shows that the mouse sperm hook (i) facilitates sperm interaction with the epithelium for better navigation and (ii) provides an anchor-like role that assists attachment of sperm to the epithelium. These results

371 suggest that the sperm hook in house mice functions to facilitate sperm migration by interacting
372 with the female reproductive tract (Firman and Simmons, 2009; Suarez, 1987; Tourmente et al.,
373 2016). We also showed that when spermatozoa swim along the uterine wall, their apical hook
374 interacts with the epithelia and determines sperm travelling direction upon encountering uterine
375 epithelium. This finding implies that the sperm hook functions as a pivot when spermatozoa
376 reach the uterine epithelium, and help spermatozoa migrate along the uterine wall by assisting in
377 pro-wall-hook sperm orientation. Additionally, the sperm hook plays an important role in
378 resisting endogenous fluid flow in the female reproductive tract by providing an anchor-like
379 function. We did not observe linkage of spermatozoa (sperm trains) that enables faster and
380 straighter swimming of the sperm train in the uterus or oviduct. Instead, we found instances of
381 the entanglement of inactive spermatozoa in the oviduct. Such aggregates of inactive
382 spermatozoa appear to obstruct the migration of other spermatozoa. However, the role that these
383 entangled spermatozoa play in sperm competition within the oviduct is a subject that necessitates
384 further investigation.

385 Previous studies using various murine rodents suggest that acquiring the ability to form sperm
386 train is a relatively rare evolutionary events in this taxon (Tourmente et al., 2016; Varea-Sánchez
387 et al., 2016). Instead of finding evidence that the sperm hook aids in sperm train formation, those
388 studies showed that variations in the length of the sperm hook, and asymmetry of sperm head
389 influenced by the sperm hook are two important variables that reflect the degree of the sperm
390 competition in murine rodents. One study even suggested that the sperm train formation (sperm
391 linkage) is independent of the existence of sperm hook (Tourmente et al., 2016). Therefore, it is
392 questionable whether acquiring the sperm hook in the murine rodents has evolved in general for
393 a better sperm linkage. In line with the previous studies, our current study also showed that
394 sperm hook plays a pivotal role in sperm-epithelium interactions by aiding sperm attachment to
395 the uterine and oviductal epithelium and influence sperm orientation during migration inside the
396 female reproductive tract (Fig 1E, F; Movie S3A, B). Such a role of the sperm hook suggests that
397 the hook facilitates interactions between sperm and epithelia of the female reproductive tract and
398 supports the migration hypothesis.

399 As we did not observe any passive sperm transfer by the internal fluid flow from the uterus to
400 intramural UTJ through the CT, it is puzzling how spermatozoa enter the intramural UTJ.
401 Although we proposed a hypothetical model of sperm passage through the CT in which the
402 sperm hook plays an important role by providing an anchor-like role that prevents backward
403 movement but allows head-forward sliding, further investigation with new experimental and
404 observational tools will be necessary. Nevertheless, our findings suggest that the CT is a key
405 female anatomical structure that controls sperm entry to the UTJ and influences sperm
406 competition. If sperm passage through the CT is too easy, associated risks such as polyspermy or
407 pathogen transmission that incur fitness costs for females also increase (Firman and Simmons,
408 2013; Mahabir et al., 2008). Therefore, the number of sperm passing through the CT should be
409 balanced by the conflict between the two sexes depending on species specific mating systems
410 and the degree of promiscuity. This conflict then gives rise to an evolutionary arms race, with
411 male's sperm fertilization ability on one side, which includes aspects such as sperm swimming
412 speed, and the female's sperm selection process on the other, which encompasses elements like
413 physio-chemical barriers in the female reproductive tract (Firman et al., 2017; Lüpold and
414 Pitnick, 2018; Simmons and Wedell, 2020). Therefore, species variations in the length of the

415 sperm hook and head asymmetry in rodents suggested in the previous studies (Tourmente et al.,
416 2016; Varea-Sánchez et al., 2016) will also reflect the mechanical and structural characteristics
417 of the CT and lumen in the intramural UTJ.

418 In the current study, we could not confirm evidence of sperm cooperation via sperm train
419 formation that aids faster sperm swimming. Instead, we discovered a new form of potential
420 sperm cooperation – synchronised sperm beating that resulted from spontaneous unidirectional
421 sperm clustering. Based on these observations, we propose that the asymmetry of the mouse
422 sperm head with apical hook plays a crucial role in synchronised sperm beating (sperm
423 cooperation) by facilitating unidirectional sperm re-arrangement at the uterine wall. The
424 asymmetrical head shape in the house mouse, therefore, may have evolved not only to facilitate
425 sperm migration but also to facilitate such sperm self-organised behaviours including
426 unidirectional clustering and following beating synchrony. Under this scenario, sperm
427 cooperation in house mice is not only mediated by sperm train formation as in some rodent
428 species (Fisher and Hoekstra, 2010; Moore et al., 2002), but mediated by the synchronised sperm
429 beating that obstruct migration of other spermatozoa in the uterus. Unidirectional sperm
430 clustering and its potential role in sperm migration were also suggested in a previous study using
431 fixed and tissue-cleared samples with in-vitro live sperm analysis (Qu et al., 2021). We could not
432 find any supporting evidence that such clustering helps sperm passage through the CT. However,
433 our observations regarding self-organised sperm behaviour provides insights into the evolution
434 of the asymmetrical structure of the sperm head in rodent species. These findings present an
435 opportunity to reconcile two hypotheses: the cooperation hypothesis (Fisher and Hoekstra, 2010;
436 Immler et al., 2007; Moore et al., 2002) and the migration hypothesis (Firman and Simmons,
437 2009; Smith and Yanagimachi, 1990).

438 The evolution of sperm characteristics, including the sperm hook, is a complex process
439 influenced by several factors. For instance, sperm competition between ejaculates is a significant
440 driving forces influencing sperm head morphology and behaviour in rodents (Fisher et al., 2014;
441 Immler et al., 2007; Tourmente et al., 2016; Varea-Sánchez et al., 2016). Cryptic female choice
442 also plays a crucial role in the evolution of sperm head shape and sperm kinetic characteristics
443 (Birkhead, 1998; Eberhard and Lehmann, 2019; Firman et al., 2017). Further investigation of
444 sperm behaviour inside the female reproductive tract or tissue mimicking microfluidic devices
445 with real-time deep tissue imaging as in the current study, will provide valuable opportunities for
446 a more comprehensive examination of both sperm-sperm and sperm-epithelium interactions in
447 the female reproductive tract. While we have focused on observing sperm interactions for only
448 natural healthy mice in this study, future works employing specifically targeted genetically
449 modified knockout animal models will further elucidate and confirm the exact genetic and
450 functional mechanisms that guide these interactions. This will help us better understand not only
451 sperm competition and cryptic female choice in mice, but also those in other animals, including
452 humans. While current assessments of sperm health generally involve measuring sperm count,
453 movement, and shape, the current study suggests that analysing interactions between
454 spermatozoa and the female reproductive tract is important and warrants further exploration.
455 Given the significance of sperm health for fertility, this work not only highlights the importance
456 of interactions between male sperm and female reproductive tract in successful migration, but
457 also opens new avenues for understanding different causes of infertility and possible targets for
458 treatment.

Materials and Methods

Custom-built two-photon microscope

To observe sperm behaviour in the female mouse reproductive organ, we built a video rate (30 frames/second at 512 x 512 pixel resolution) Two-Photon Laser Scanning Fluorescence Microscope (2PLSM; Fig. S1). A tunable femtosecond pulse laser (Chameleon, Discovery) was tuned to a choice of wavelengths from 960, 970, 980 and 1000 nm to simultaneously excite GFP and Ds-Red for sperm imaging and for autofluorescence imaging of the reproductive tract. Imaging quality was found to be similar for these wavelength ranges. All images were taken using a water dipping low magnification high NA objective lens (Nikon 16X, 0.8NA). Video-rate imaging was achieved using a resonant Galvo scanning mirror system oscillating at 8 kHz. The laser power was actively controlled using a Pockels cell. Synchronization between the Galvos, sample/objective stages, Pockels cell, photomultiplier tubes (PMTs), and the data acquisition systems were controlled using ScanImage, ver. SI2021.1.0 (Pologruto et al., 2003).

Mice preparation and mating

We used two male transgenic mice lines for mating experiments. We purchased B6D2-Tg(CAG/Su9-DsRed2, Acr3-EGFP)RBGS002Osb male mice that express DsRed in the mitochondria at sperm midpiece and EGFP in the sperm acrosome from Riken BRC, Japan, depositor: M. Ikawa (Hasuwa et al., 2010). We then conducted in vitro fertilization to produce specific pathogen-free (SPF) F1 mice. The fertilized eggs (2-cell stage embryos) were then artificially inseminated into SPF wild-type C57BL/6J females. After we confirmed successful production of transgenic F1 male mice by PCR, we confirmed the SPF status and formed two breeding colonies with the transgenic F1 males under the SPF condition. One breeding colony comprised two wild-type C57BL/6J females to better reproduce F2 generation. We also made breeding colonies that consisted of a transgenic C57BL/6J female, Cx3cr1tm2.1(cre/ERT2)Litt/WganJ (JAX stock #021160, Cx3cr1 female) that expresses EYFP in microglia (Parkhurst et al., 2013) to test whether sperm functionality changes in other mice including double-transgenic mice. When F2 mice got older than 6 weeks, they were transferred to another room where mating experiments were conducted. After transfer, each male mouse for mating experiments was single-caged. We used the F2 males that derived from both colonies that had the two genes (CAG/Su9-DsRed2 and Acr3-EGFP; RBGS male) or three genes (CAG/Su9-DsRed2, Acr3-EGFP, and Cx3cr1; RBGS-Cx3cr1 male) for mating experiments. We could not find any phenotypic difference in the sperm of the two strains – sperm from both strains expressed red fluorescence at the midpiece and green fluorescence at the acrosome at the head. We confirmed that both strains of F2 males were fertile, and their sperm also successfully migrated through the female reproductive tract, from the uterus to the ampulla.

In total, we used 3 males that successfully mated with females due to space limits in the experimental room (Table S1). The 3 males were used repeatedly for all mating experiments in the current study except one vasectomized RBGS-Cx3cr1 male that was used only once for comparison of the CT structure for virgin and non-virgin female mice (Table S2). All mice were kept under a housing condition that allows free access to food and water with 12 hours of light and dark cycle (lighting from 6 to 18 o'clock, dark from 18 to 6 o'clock). Mating experiments

were done under light conditions from 9 am to 12 pm for three hours. Oestrus was induced by exposing male bedding materials (wood shavings) that consisted of male excretion to females older than 8 weeks. Three to seven days after exposure to the bedding materials, oestrus was checked daily following previously established protocols (Byers et al., 2012). When we found oestrous females, we relocated one or two females to a single-caged male. When males showed no interest in the female (no mounting attempts) or the female rejected the male's mounting attempt for the first 10 minutes, we returned the female to its original cage. The returned females were not exposed to other males until the next mating trial on the next day or one week later. All females in the experiments had no birth records before successful copulatory plug-confirmed mating. However, some of them probably had multiple oestrous cycles given our multiple oestrus-inducing trials. We did not limit the age of females and males for our experiments to minimize the number of sacrificed animals. We observed the male's mating until we could observe ejaculation. To confirm male ejaculation, we checked the copulatory plug from the female genitalia after we observed ejaculatory behaviour – the male stops thrusting and holds the female for about 5 to 10 seconds when it ejaculates. After this ejaculatory behaviour, we waited for 2 minutes and if the male did not exhibit further mounting, we checked the copulatory plug from the female genitalia. When the male ejaculated, we kept them together for up to 3 hours then took out the female for imaging experiments.

Ex vivo imaging with two-photon microscopy

Female mice were sacrificed by cervical dislocation after anaesthesia using 2% isoflurane inhalation which usually took less than 5 minutes. After euthanasia, the female reproductive tract with the copulatory plug was excised and washed with Dulbecco's modified Eagle's medium (Tayama et al., 2006) (DMEM; GibcoTM, cat. No. 21063029). After washing, the reproductive tract was attached to a tissue culture dish with tissue adhesive (3M Vetbond 1469SB). After attachment, we filled the dish with 37°C preheated medium that contained an equal amount of DMEM and modified human tubal fluid (mHTF; Fujifilm Irvine Scientific, cat. ID. 90126) medium. All media were stored for at least 1 hour in a 37°C preheated incubator with 5% of CO_2 concentration before use. The culture dish was then placed on the 37°C preheated metal mount of the two-photon microscope and imaged with varying laser power for different depths. Most of the images were taken with 512 x 512 pixel image size at 30 fps (262,144 pixels per frame). Multicolour imaging was performed where each frame of the image has two colour channels (red and green). If needed, we could increase the frame rate up to 110 fps or higher by reducing the acquired image size to 128 x 128 (16,384 pixels per frame). We conducted observation for about 3 to 6 hours. During our observation, the uterus continued contraction and relaxation cycles.

To image the entire depth of the reproductive tract, we applied tissue clearing to investigate the structure of the UTJ entrance (or colliculus tubarius, CT) using the C-Match solution (RI = 1.46, Crayon technologies, Korea). In brief, the tissue was first washed 3 times in PBS and fixed in 4% paraformaldehyde for 3 hours at 4°C in a refrigerator. After fixation, we washed the tissue 3 times with PBS and the absorbed residual PBS using paper towels. We then added C-Match to the sample and waited overnight and imaged it on the next day with the sample submerged in C-Match. We imaged three cleared samples from three different females. In one sample (Figure 3A), only the intramural UTJ part was excised from one unmated transgenic C57BL/6J female mouse – a hybrid female that was delivered from Cx3cr1 female and Thy1 male (JAX stock

543 #030526) called Tg(Thy1-jRGECO1a)GP8.31Dkim (Dana et al., 2018). Another sample was
544 from a female that was mated with a vasectomized RBGS-Cx3cr1 male. In this sample, the
545 whole female reproductive tract was excised with the copulatory plug, so the intramural UTJ was
546 covered by the uterus. This sample was used to compare the UTJ for virgin and non-virgin
547 females. The final sample was from a wild-type female that was mated with an RBGS-Cx3cr1
548 male. For cleared tissue imaging, we acquired 3D volume images with 2 um Z-axis step size
549 while averaging 20 (first sample) or 30 images (second sample) per slice to increase the signal to
550 noise ratio using autofluorescence of the reproductive tract tissue.

551 ***Sperm tracking and speed measurement***

552 We used Fiji (Schindelin et al., 2012) to process acquired images and its plugin, called
553 TrackMate (Ershov et al., 2022; Tinevez et al., 2017) to track sperm trajectory in the uterus. We
554 extracted trajectories from 60 sequential images (duration 2 seconds) for sperm tracking when
555 uterus movement was the smallest. We also used Turboreg (Thevenaz et al., 1998), an ImageJ
556 plugin, to realign the images when there was a shift between images due to uterine movement.
557 Additionally, out of eight stacked images, we cropped three to obtain a straight view of the
558 uterine wall. After preparing the images, we targeted the sperm head to track sperm as the sperm
559 head expressed EGFP which was easy to track. We used Thresholding Detector to select sperm
560 heads and LAP Tracker to trace sperm trajectories using the TrackMate plugin. We also adjusted
561 parameter values in the plugin to better select sperm trajectories. Our final parameter values are
562 as follows: head radius (> 0.75 μm), frame-to-frame linking (10 ~ 11 μm), track segment gap
563 closing (max distance: 10 ~ 11 μm, max frame gap: 2), number of spots in track (> 6), and max
564 distance travel (2.5 μm). When there were artificial trajectories that were not from sperm, we
565 manually removed the track. If the original parameters could not detect well or had too many
566 false tracks, we adjusted two parameters; frame-to-frame linking (up to 12 μm), and track
567 segment gap closing (only max distance up to 12 μm). We also tracked the trajectories of sperm
568 trains using the same parameters and settings. However, to reduce computation time and prevent
569 mis-tracking of non-sperm cells, we cropped the images and utilized 100x100 pixel images that
570 contain the entire trajectory of each sperm train as well as other unlinked single spermatozoa.

571 To calculate sperm speed in relation to the distance from the uterine wall, we need to define the
572 uterine wall. To define the uterine wall, we first selected images with straighter uterine wall and
573 projected the extracted 60 sequential images into one plane by taking the maximum intensity
574 projection with some adjustment of brightness and contrast using Fiji. For some images taken at
575 a low magnification level that contained curved uterine walls, we used parts of the field of view
576 that contained straight walls appropriate for our analysis. Next, we used the object selection tool
577 of Adobe Photoshop CC (23.1.0 version) to automatically select the walls from the projected
578 images. We then extracted the uterine wall image layer and pasted it to a blank image with white
579 background. Finally, we extracted the wall coordinates by selecting the non-zero-valued pixels
580 that formed the boundary of the uterine wall (blue coloured area in Fig. S2A). The boundary
581 coordinates were converted to a micrometre scale based on the magnification and image
582 resolution to normalize the units between different images obtained with different magnification
583 factors. We fitted the uterine wall coordinates using linear regression. The fitted linear regression
584 line was considered the uterine wall of each female (① in Fig. S2B) and used to calculate the
585 distance and angle (radian) between sperm and the wall.

586 We measured the distance between sperm and the uterine wall by calculating the minimum
587 distance between the mid-point of each sperm trajectory and the fitted line of the uterine wall
588 (② in Fig. S2B). The angle between a sperm trajectory and the uterine wall was calculated by
589 measuring the angle between the fitted line and a straight line that passed the first and last spots
590 of the trajectory (③ in Fig. S2B). We then computed sperm progression speed parameters used
591 in CASA (Amann and Waberski, 2014) using our sperm tracking data using the TrackMate plug-
592 in. We first calculated curvilinear velocity, VCL by dividing the total distance travelled (μm) by
593 total track time – the time (second) taken from the first point (spot) to the last point in a sperm
594 trajectory. The straight line velocity, VSL was calculated by dividing the track displacement –
595 the distance between the first and last spots of a sperm trajectory – by the total track time
596 (second). We also calculated the linearity of forward progression, LIN of sperm by dividing VSL
597 by VCL (range 0 to 1). Along with the above CASA-used parameters, we defined a new
598 parameter, the straight line-to-sideward movement ratio (SWR) to estimate sperm migration
599 linearity by comparing forward and sideward moving distances. SWR was calculated by dividing
600 the track displacement (μm) of a sperm trajectory by the maximum sideward movement distance
601 (μm) – the maximum distance between two parallel lines passing each point (spot) that parallel
602 to the track displacement line (④ in Fig. S2B). Further information on the terms and parameters
603 of the TrackMate plug-in used in the current paper is also described in a paper and manual by the
604 developers (Ershov et al., 2022; Tinevez et al., 2017).

605 ***Statistical analysis***

606 All statistical analyses were done using R, version 4.3.0 (R Core Team, 2023). To estimate
607 sperm swimming speed and linearity in relation to the uterine wall, we used data from 8
608 copulation experiments between 8 females and 3 males. We ran 4 generalized linear mixed
609 models to test whether sperm move faster and straighter when they migrate along the uterine
610 wall. We used log-transformed VCL, VSL, LIN, and SWR as response variables in each model.
611 In all models, we included the angle and distance between the wall and sperm trajectories as
612 explanatory variables. We also included whether we cropped the image or not (O or X) to check
613 the effect of image cropping on the analysis. Male IDs and the date of experiments were included
614 as random effects in all models to control possible individual variations in sperm and
615 reproductive tract properties. All models did not violate assumptions. All full models were also
616 compared with null models that only included random effect and all full models were
617 significantly better than the null models. All variance influencing factors (VIFs) were less than
618 1.1 which indicates no serious drawback from collinearity.

619 **References**

620 Alvarez L, Friedrich BM, Gompper G, Kaupp UB. 2014. The computational sperm cell. *Trends Cell Biol* **24**:198–
621 207. doi:10.1016/j.tcb.2013.10.004

622 Amann RP, Waberski D. 2014. Computer-assisted sperm analysis (CASA): capabilities and potential developments.
623 *Theriogenology* **81**:5–17. doi:10.1016/j.theriogenology.2013.09.004

624 Anderson MJ, Nyholt J, Dixson AF. 2005. Sperm competition and the evolution of sperm midpiece volume in
625 mammals. *J Zool* **267**:135–142. doi:10.1017/S0952836905007284

626 André GI, Firman RC, Simmons LW. 2020. Baculum shape and paternity success in house mice: evidence for
627 genital coevolution. *Philos Trans R Soc B Biol Sci* **375**:20200150. doi:10.1098/rstb.2020.0150

Baker RR, Bellis MA. 1993. Human sperm competition: ejaculate manipulation by females and a function for the female orgasm. *Anim Behav* **46**:887–909. doi:10.1006/anbe.1993.1272

Benninger RKP, Piston DW. 2013. Two-photon excitation microscopy for the study of living cells and tissues. *Curr Protoc Cell Biol* **59**:4111–41124. doi:10.1002/0471143030.cb0411s59

Birkhead TR. 1998. Cryptic female choice: criteria for establishing female sperm choice. *Evolution* **52**:1212–1218. doi:10.1111/j.1558-5646.1998.tb01848.x

Breed WG. 2004. The spermatozoon of Eurasian murine rodents: its morphological diversity and evolution. *J Morphol* **261**:52–69. doi:10.1002/jmor.10228

Byers SL, Wiles MV, Dunn SL, Taft RA. 2012. Mouse estrous cycle identification tool and images. *PLOS ONE* **7**:e35538. doi:10.1371/journal.pone.0035538

Dana H, Novak O, Guardado-Montesino M, Fransen JW, Hu A, Borghuis BG, Guo C, Kim DS, Svoboda K. 2018. Thy1 transgenic mice expressing the red fluorescent calcium indicator jRGECO1a for neuronal population imaging in vivo. *PLOS ONE* **13**:e0205444. doi:10.1371/journal.pone.0205444

Díaz-García C, Akhi SN, Martínez-Varea A, Brännström M. 2013. The effect of warm ischemia at uterus transplantation in a rat model. *Acta Obstet Gynecol Scand* **92**:152–159. doi:10.1111/aogs.12027

Eberhard WG. 1996. Female control: sexual selection by cryptic female choice. Princeton University Press. doi:10.2307/j.ctvs32rx1

Eberhard WG, Lehmann GUC. 2019. Demonstrating sexual selection by cryptic female choice on male genitalia: what is enough? *Evolution* **73**:2415–2435. doi:10.1111/evo.13863

Elgeti J, Kaupp UB, Gompper G. 2010. Hydrodynamics of sperm cells near surfaces. *Biophys J* **99**:1018–1026. doi:10.1016/j.bpj.2010.05.015

Ershov D, Phan M-S, Pylvänäinen JW, Rigaud SU, Le Blanc L, Charles-Orszag A, Conway JRW, Laine RF, Roy NH, Bonazzi D, Duménil G, Jacquemet G, Tinevez J-Y. 2022. TrackMate 7: integrating state-of-the-art segmentation algorithms into tracking pipelines. *Nat Methods* **19**:829–832. doi:10.1038/s41592-022-01507-1

Firman RC, Gasparini C, Manier MK, Pizzari T. 2017. Postmating female control: 20 years of cryptic female choice. *Trends Ecol Evol* **32**:368–382. doi:10.1016/j.tree.2017.02.010

Firman RC, Simmons LW. 2013. Sperm competition risk generates phenotypic plasticity in ovum fertilizability. *Proc R Soc B Biol Sci* **280**:20132097. doi:10.1098/rspb.2013.2097

Firman RC, Simmons LW. 2009. Sperm competition and the evolution of the sperm hook in house mice. *J Evol Biol* **22**:2505–2511. doi:10.1111/j.1420-9101.2009.01867.x

Fisher HS, Giomi L, Hoekstra HE, Mahadevan L. 2014. The dynamics of sperm cooperation in a competitive environment. *Proc R Soc B Biol Sci* **281**:20140296. doi:10.1098/rspb.2014.0296

Fisher HS, Hoekstra HE. 2010. Competition drives cooperation among closely related sperm of deer mice. *Nature* **463**:801–803. doi:10.1038/nature08736

Greff JM, Parker GA. 2000. Spermicide by females: what should males do? *Proc R Soc Lond B Biol Sci* **267**:1759–1763. doi:10.1098/rspb.2000.1207

Hasuwa H, Muro Y, Ikawa M, Kato N, Tsujimoto Y, Okabe M. 2010. Transgenic mouse sperm that have green acrosome and red mitochondria allow visualization of sperm and their acrosome reaction *in vivo*. *Exp Anim* **59**:105–107. doi:10.1538/expanim.59.105

Helmchen F, Denk W. 2005. Deep tissue two-photon microscopy. *Nat Methods* **2**:932–940. doi:10.1038/nmeth818

Hino T, Yanagimachi R. 2019. Active peristaltic movements and fluid production of the mouse oviduct: their roles in fluid and sperm transport and fertilization. *Biol Reprod* **101**:40–49. doi:10.1093/biolre/ioz061

Holman L, Snook RR. 2008. A sterile sperm caste protects brother fertile sperm from female-mediated death in *Drosophila pseudoobscura*. *Curr Biol* **18**:292–296. doi:10.1016/j.cub.2008.01.048

Holman L, Snook RR. 2006. Spermicide, cryptic female choice and the evolution of sperm form and function. *J Evol Biol* **19**:1660–1670. doi:10.1111/j.1420-9101.2006.01112.x

Hook KA, Wilke LM, Fisher HS. 2021. Apical sperm hook morphology is linked to sperm swimming performance and sperm aggregation in *Peromyscus* mice. *Cells* **10**:2279. doi:10.3390/cells10092279

Immler S, Moore HDM, Breed WG, Birkhead TR. 2007. By hook or by crook? Morphometry, competition and cooperation in rodent sperm. *PLOS ONE* **2**:e170. doi:10.1371/journal.pone.0000170

Ishikawa Y, Usui T, Yamashita M, Kanemori Y, Baba T. 2016. Surfing and swimming of ejaculated sperm in the mouse oviduct. *Biol Reprod* **94**. doi:10.1095/biolreprod.115.135418

Kantsler V, Dunkel J, Blayney M, Goldstein RE. 2014. Rheotaxis facilitates upstream navigation of mammalian sperm cells. *eLife* **3**:e02403. doi:10.7554/eLife.02403

Keller PJ. 2013. Imaging morphogenesis: technological advances and biological insights. *Science* **340**:1234168. doi:10.1126/science.1234168

Koprowski JL. 1992. Removal of copulatory plugs by female tree squirrels. *J Mammal* **73**:572–576. doi:10.2307/1382026

Lange R, Reinhardt K, Michiels NK, Anthes N. 2013. Functions, diversity, and evolution of traumatic mating. *Biol Rev* **88**:585–601. doi:10.1111/brv.12018

Lüpold S, Pitnick S. 2018. Sperm form and function: what do we know about the role of sexual selection? *Reproduction* **155**:R229–R243. doi:10.1530/REP-17-0536

Mahabir E, Bauer B, Schmidt J. 2008. Rodent and germplasm trafficking: risks of microbial contamination in a high-tech biomedical world. *ILAR J* **49**:347–355. doi:10.1093/ilar.49.3.347

Mangels R, Tsung K, Kwan K, Dean MD. 2016. Copulatory plugs inhibit the reproductive success of rival males. *J Evol Biol* **29**:2289–2296. doi:10.1111/jeb.12956

Moore H, Dvoráková K, Jenkins N, Breed W. 2002. Exceptional sperm cooperation in the wood mouse. *Nature* **418**:174–177. doi:10.1038/nature00832

Nakanishi T, Isotani A, Yamaguchi R, Ikawa M, Baba T, Suarez SS, Okabe M. 2004. Selective passage through the uterotubal junction of sperm from a mixed population produced by chimeras of calmegin-knockout and wild-type male mice. *Biol Reprod* **71**:959–965. doi:10.1095/biolreprod.104.028647

Parker GA. 1970. Sperm competition and its evolutionary consequences in the insects. *Biol Rev* **45**:525–567. doi:10.1111/j.1469-185X.1970.tb01176.x

Parkhurst CN, Yang G, Ninan I, Savas JN, Yates JR, Lafaille JJ, Hempstead BL, Littman DR, Gan W-B. 2013. Microglia promote learning-dependent synapse formation through brain-derived neurotrophic factor. *Cell* **155**:1596–1609. doi:10.1016/j.cell.2013.11.030

Pologruto TA, Sabatini BL, Svoboda K. 2003. ScanImage: flexible software for operating laser scanning microscopes. *Biomed Eng OnLine* **2**:13. doi:10.1186/1475-925X-2-13

Qu Y, Chen Q, Guo S, Ma C, Lu Y, Shi J, Liu S, Zhou T, Noda T, Qian J, Zhang L, Zhu X, Lei X, Cao Y, Li W, Li W, Plachta N, Matzuk MM, Ikawa M, Duan E, Zhang Y, Wang H. 2021. Cooperation-based sperm clusters mediate sperm oviduct entry and fertilization. *Protein Cell* **12**:810–817. doi:10.1007/s13238-021-00825-y

R Core Team. 2024. R: A language and environment for statistical computing.

R Core Team. 2023. R: A language and environment for statistical computing.

Roberts EK, Lu A, Bergman TJ, Beehner JC. 2012. A Bruce effect in wild Geladas. *Science* **335**:1222–1225. doi:10.1126/science.1213600

Roldan ERS, Gomendio M, Vitullo AD. 1992. The evolution of eutherian spermatozoa and underlying selective forces: female selection and sperm competition. *Biol Rev* **67**:551–593. doi:10.1111/j.1469-185X.1992.tb01193.x

Schindelin J, Arganda-Carreras I, Frise E, Kaynig V, Longair M, Pietzsch T, Preibisch S, Rueden C, Saalfeld S, Schmid B, Tinevez J-Y, White DJ, Hartenstein V, Eliceiri K, Tomancak P, Cardona A. 2012. Fiji: an open-source platform for biological-image analysis. *Nat Methods* **9**:676–682. doi:10.1038/nmeth.2019

Simmons LW, Wedell N. 2020. Fifty years of sperm competition: the structure of a scientific revolution. *Philos Trans R Soc B Biol Sci* **375**:20200060. doi:10.1098/rstb.2020.0060

Smith TT, Yanagimachi R. 1990. The viability of hamster spermatozoa stored in the Isthmus of the oviduct: the importance of sperm-epithelium contact for sperm survival. *Biol Reprod* **42**:450–457. doi:10.1095/biolreprod42.3.450

Suarez SS. 1987. Sperm transport and motility in the mouse oviduct: observations in situ. *Biol Reprod* **36**:203–210. doi:10.1095/biolreprod36.1.203

Sutter A, Lindholm AK. 2016. The copulatory plug delays ejaculation by rival males and affects sperm competition outcome in house mice. *J Evol Biol* **29**:1617–1630. doi:10.1111/jeb.12898

Tayama K, Fujita H, Takahashi H, Nagasawa A, Yano N, Yuzawa K, Ogata A. 2006. Measuring mouse sperm parameters using a particle counter and sperm quality analyzer: a simple and inexpensive method. *Reprod Toxicol* **22**:92–101. doi:10.1016/j.reprotox.2005.11.009

Thevenaz P, Ruttimann UE, Unser M. 1998. A pyramid approach to subpixel registration based on intensity. *IEEE Trans Image Process* **7**:27–41. doi:10.1109/83.650848

Tinevez J-Y, Perry N, Schindelin J, Hoopes GM, Reynolds GD, Laplantine E, Bednarek SY, Shorte SL, Eliceiri KW. 2017. TrackMate: an open and extensible platform for single-particle tracking. *Methods*, Image Processing for Biologists **115**:80–90. doi:10.1016/j.ymeth.2016.09.016

Tourmente M, Zarka-Trigo D, Roldan ERS. 2016. Is the hook of muroid rodent's sperm related to sperm train formation? *J Evol Biol* **29**:1168–1177. doi:https://doi.org/10.1111/jeb.12857

Varea-Sánchez M, Tourmente M, Bastir M, Roldan ERS. 2016. Unraveling the sperm bauplan: relationships between sperm head morphology and sperm function in rodents. *Biol Reprod* **95**:25, 1–9. doi:10.1095/biolreprod.115.138008

Yu S-X, Wu Y, Luo H, Liu Y, Chen Y-C, Wang Y-J, Liu W, Tang J, Shi H, Gao H, Jing G, Liu Y-J. 2023. Escaping behavior of sperms on the biomimetic oviductal surface. *Anal Chem* **95**:2366–2374. doi:10.1021/acs.analchem.2c04338

Zaferani M, Palermo GD, Abbaspourrad A. 2019. Strictures of a microchannel impose fierce competition to select for highly motile sperm. *Sci Adv* **5**:eaav2111. doi:10.1126/sciadv.aav2111

Acknowledgments

We appreciate members of the Bio-Optics Lab and In-vivo Research Center at the Ulsan National Institute of Science and Technology for their help in building and maintaining microscopy instruments and mouse strains; particularly I. Kim, S. Park, Y. Lee, Y. Kwon, Y. Choi, H. Kim, E. Cho, and T. Asadishad. We also thank M. Okabe, G. Kang, and Y. Kawaguchi for their comments about the methods and manuscript. **Funding sources**: National Research Foundation of Korea grant 2020R1A6A3A01098226 (HR), National Research Foundation of Korea grant 2019M3E5D2A01063812 (JP), National Research Foundation of Korea grant 2021R1A2C3012903 (JP), National Research Foundation of Korea grant 2021R1A4A1031644 (JP), National Research Foundation of Korea grant RS-2023-00264980 (JP), Ministry of Science and ICT (IITP-2023-RS-2023-00259676) (JP), National Research Foundation of Korea grant 2021M3A9G8022960 (JK1, Jae-Ick Kim), National Research Foundation of Korea grant 2022M325E8017907 (JK1)

Author Contributions

Conceptualization: HR, JP, Methodology: HR, KN, YJ, SL, JK2 (Jungmo Kim), JP, Investigation: HR, KN, BL, YJ, JP, Visualization: HR, KN, YJ, JP, Funding acquisition: HR, JK1, JP, Project administration: JK1, JP, Supervision: JK1, JP, Writing – original draft: HR, JP, Writing – review & editing: all authors

Declaration of interests

Authors declare that they have no competing interests.

Data and materials availability

Raw data on sperm trajectories in the female reproductive track is available at https://figshare.com/s/82d3f991ba884af73898. Custom codes for sperm tracking data analysis written with Matlab (version R2019b) are available at https://github.com/YundonJeong/Sperm_tracking.